Journal of Inorganic Biochemistry 165 (2016) 36–48

Contents lists available at ScienceDirect

Journal of Inorganic Biochemistry

journal homepage: www.elsevier.com/locate/jinorgbio

Coordination ability and biological activity of a naringenin thiosemicarbazone

Katarzyna Brodowska [a], Isabel Correia [b], Eugenio Garribba [c], Fernanda Marques [d], Elżbieta Klewicka [a], Elżbieta Łodyga-Chruscińska [a,*], João Costa Pessoa [b,*], Aliaksandr Dzeikala [a], Longin Chrusciński [e]

[a] Faculty of Biotechnology and Food Chemistry, Lodz University of Technology, Stefanowskiego Street 4/10, 90-924 Lodz, Poland
[b] Centro de Química Estrutural, Instituto Superior Técnico, Universidade de Lisboa, Av. Rovisco Pais, 1049-001 Lisboa, Portugal
[c] Dipartimento di Chimica e Farmacia, Università di Sassari, via Vienna 2, I-07100 Sassari, Italy
[d] Centro de Ciências e Tecnologias Nucleares, Instituto Superior Técnico, Universidade de Lisboa, Estrada Nacional 10 (km 139.7), 2695-066 Bobadela LRS, Portugal
[e] Faculty of Process an Environmental Engineering, Lodz University of Technology, Wolczanska 175, 90-924 Lodz, Poland

ARTICLE INFO

Article history:
Received 10 June 2016
Received in revised form 18 September 2016
Accepted 29 September 2016
Available online 30 September 2016

Keywords:
Naringenin
Thiosemicarbazones
Schiff bases
Copper complexes
HSA
DNA

ABSTRACT

The present work is devoted to reveal physicochemical properties and several biological actions of a new thiosemicarbazone (NTSC) derived from naringenin, a natural flavanone, and its Cu-complexes formed in mixed solvent solutions. Equilibrium solution studies were carried out on the NTSC and Cu-NTSC complexes in DMSO/water mixture. The proton-dissociation constants of the ligand, the stability constants and the coordination modes of the metal complex species were determined by means of pH-potentiometric, UV–vis and EPR methods. Mono- and bis-ligand complexes in different protonation states were identified. Circular dichroism, fluorimetric and gel electrophoresis studies demonstrated that both NTSC and copper complex interact with CT DNA and plasmid pEGFP-C1. Fluorimetric experiments allowed to confirm that both NTSC and its Cu(II)-complex bind to human serum albumin (HSA), the Cu-NTSC giving a stronger quenching effect than NTSC at similar molar ratios. Investigations of antibacterial and antifungal properties were carried out on selected strains of bacteria and fungi. The cytotoxic effects were studied on the cancer A2780 and the non-cancer HEK cells, both compounds being found non-toxic.

1. Introduction

Semicarbazides and thiosemicarbazides are compounds that when binding metal ions may give rise to a great variety of coordination modes, this having a significant impact on the biological properties of both metal ion and ligand [1]. On the other hand, natural flavonoids are polyphenolic compounds, which, due to their broad pharmacological applications, have been arising much research interest. They are present in fruits and plants and have beneficial health effects, as reported in several studies [2–5]. Namely, flavanones, a subclass of flavonoids, exhibit anti-oxidant, chemopreventive, anti-cancer, antiviral, anti-bacterial, as well as immunomodulatory [4] and estrogenic effects [6–8].

Schiff base compounds and their metal-complexes have been extensively explored as therapeutic drugs [9–13], but to date, Schiff base ligands derived from the reaction of flavonoids and thiosemicarbazides are underexplored. Thiosemicarbazone Schiff bases, as well as their metal complexes, are a class of compounds with relevant medicinal and pharmaceutical applications [1,14]. Regardless of the extensive amount of data on the biological effects of thiosemicarbazones and their metal complexes, there are still many unknown aspects about their mechanism of action and potential application. Thus, further studies are justified and required to explain the observed phenomena, deepen the present knowledge in this field and explore new areas of use. Flavonoids and thiosemicarbazones can coordinate to metal ions and this binding can affect their biological effects and mechanisms of action [15–22]. Several Cu(II)- and $V^{IV}O$-flavonoid complexes revealed interesting biological properties [15–25]. Similarly the hydrazone hesperetin Schiff base (HHSB) and its Cu(II)-complex [20–22] were reported. The complex Cu-HHSB showed stronger intercalative binding to DNA and higher oxidative activity than HHSB. Moreover, HHSB and Cu-HHSB display antimicrobial effects against tested strains of bacteria. The antimicrobial activity and mechanism of action of these compounds require further study to get more information on the biological significance of the hydrazone Schiff bases and the role of Cu(II) ions bound to them.

The synthesis of a new thiosemicarbazone derived from naringenin (NTSC, Scheme 1), a natural flavanone, and of its Cu-complex, their antioxidant and calf thymus DNA binding properties were investigated and recently reported in a previous publication by some of us [26]. The present work reports physicochemical properties and several biological effects of NTSC and its Cu(II)-complexes formed in mixed-

* Corresponding authors.
E-mail addresses: elalodyg@p.lodz.pl (E. Łodyga-Chruscińska), joao.pessoa@ist.utl.pt (J.C. Pessoa).

http://dx.doi.org/10.1016/j.jinorgbio.2016.09.014
0162-0134/

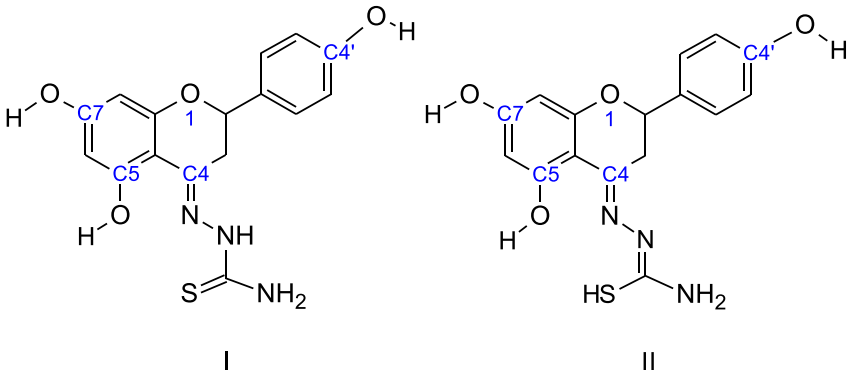

Scheme 1. Tautomers of (±)-2-[5,7-dihydroxy-2-(4-hydroxyphenyl)-2,3-dihydro-4H-chromen-4-ylidene]hydrazinecarbothioamide (NTSC).

solvent solutions. The speciation of ligand and Cu(II)-complexes, especially at physiological pH, can provide information concerning which is the chemical form of the complex in biological media, and this can contribute to a better understanding of their biological activity [27,28]. Copper is an essential element, and many of its complexes have been found appropriate for biological applications due to their binding ability and redox properties. Many Cu(II)-complexes of heterocyclic bases have been shown to depict cytotoxic activities and there are several reports of their interaction with DNA and action as artificial nucleases. Some of Cu(II) complexes with Schiff bases show anti-bacterial and anti-proliferative effects. [22,29–32] Serum protein binding is recognized as a crucial factor in the in vivo performance of drugs [33–37]. Albumin, namely human serum albumin (HSA) has multiple specific and non-specific binding sites where a large number of endogenous and exogenous substances bind. For any type of prospective drug, namely a metal complex, the knowledge of the nature and strength of its binding to HSA is very important to evaluate how it is transported in blood and up-taken by the target cells/tissues. A few studies have been done regarding the binding of flavonoid Cu(II)- and $V^{IV}O$-complexes to albumins using fluorescence spectroscopy. This method gives an indirect measurement of the binding of a drug to HSA, normally the quenching of Trp residues, but it is a very practical and straightforward method to probe the binding. The determination of the value of the apparent binding constant K_{BC} is relevant to understand the distribution of the drug in plasma. A weak binding allows higher concentrations of the compound in plasma, and leads to a short lifetime or poor distribution of the drug, while a relatively strong binding produces a decrease of concentrations in plasma improving the distribution and the pharmacological effect of the compound [38].

NTSC and its Cu(II)-complexes are only slightly soluble in water and therefore equilibrium solution studies were carried out on the complexes of NTSC with Cu(II) in dimethylsulfoxide (DMSO)/water mixtures by means of pH-potentiometric, UV–vis and EPR methods. To allow a better understanding of their potential biological effects, the studies of the interactions of the ligand and the complex with HSA and with DNA were undertaken using spectroscopic and electrophoretic techniques. Experiments accessing their antibacterial, antifungal and cytotoxic properties have been also carried out and are reported.

2. Experimental

2.1. Materials

The racemic naringenin, thiosemicarbazide, NaOH, KCl, KNO_3, $CuCl_2$, $Cu(NO_3)_2$ and all other compounds were purchased from Sigma-Aldrich Co. All reagents were of analytical quality and were used without further purification. The synthesis of (±)-2-[5,7-dihydroxy-2-(4-hydroxyphenyl)-2,3-dihydro-4H-chromen-4-ylidene]hydrazinecarbothioamide (NTSC) and the solid complex corresponding to a formulation: $[Cu(LH_3)(OAc)]\cdot H_2O$ denoted as CuNTSC in this work were prepared in accordance to the procedure described in our previous publication [26]. The Cu(II) stock solutions were prepared by dissolving anhydrous $Cu(NO_3)_2$ or $CuCl_2$ in the exact amount of HNO_3 or HCl. The metal concentration was determined by complexometric titration with EDTA. Accurate acid concentration in the Cu(II) stock solution was determined by pH-potentiometric titration. The NTSC stock solutions were determined by the Gran's method [39].

2.2. Methods of analysis

Elemental analysis (C, H, N and S) was carried out using EuroVector 3018 analyzer (see SI). The metal content of the complex was determined using atomic absorption spectrometer: AAS GBC 932 Plus (GBC Scientific Equipment Ltd., Australia) with copper hollow cathode lamp. The melting point of NTSC was determined with an Electrothermal 9200 microscopic melting point apparatus. The IR spectra were recorded employing a Nicolet 6700 (Thermo-Scientific) FT-IR spectrometer, in the 4500–500 cm^{-1} region. ^1H NMR spectra were recorded on a Bruker AV200 200MH spectrometer in DMSO-d_6 with TMS (tetramethylsilane) as internal standard. Mass spectra were done with a Finnigan MAT 9 instrument. EPR spectra were recorded with an X-band (9.4 GHz) Bruker EMX spectrometer equipped with an HP 53150A microwave frequency counter. The circular dichroism (CD) spectra were recorded on a Jasco J-720 spectropolarimeter with the UV–vis (200–700 nm) photomultiplier (EXEL-308). For the solutions containing HSA, the UV–visible absorption (UV–vis) spectra were recorded on a Perkin-Elmer Lambda 35 spectrophotometer and the fluorescence spectra were measured on Horiba Jobin Yvon fluorescence spectrometer model FL 1065. For the solutions containing DNA, the UV absorption spectra were recorded on a Perkin-Elmer Lambda 11 spectrophotometer, and the fluorescence spectra on a Hitachi Fluorescence Spectrophotometer F-2000.

2.2.1. Potentiometry

The pH-potentiometric measurements for determination of the protonation constants of the ligand and the overall stability constants of the metal complexes were carried out at an ionic strength of 0.10 M KNO_3 at 25.0 ± 0.1 °C in DMSO/water (30%:70%, v/v) as solvent. The titrations were done with carbonate-free NaOH solution of accurately known concentration (ca. 0.1 M). The concentrations of the base and HNO_3 solutions were determined by pH-potentiometric titrations. Measurements were carried out with a MOLSPIN pH meter (Molspin Ltd., Newcastle-upon-Tyne, UK) equipped with a digitally operated syringe (the Molspin DSI 0.250 mL) computer controlled, using a Russel CMAWL/S7 semi-micro combined electrode. The electrode system was calibrated according to Irving et al. [40] and the pH-metric readings could therefore be converted into hydrogen-ion concentrations. The average water-ionization constant, pK_w, is 14.52 ± 0.05 with DMSO:water (30:70, v/v) as solvent [41]. The samples were deoxygenated by

bubbling purified argon for ca. 10 min prior to the measurements, as well as during the titrations. The pH-metric titrations were carried out in the pH range 2.0–12.0 and the initial volume of the samples was 2.0 mL. The ligand concentration was 1×10^{-3} M and metal:ligand ratios of 1:1 and 1:2 were used. The accepted fitting of the titration curves was always <0.01 mL. The number of experimental points was within 100–150 for each titration curve. The reproducibility of the titration points included in the evaluation was within 0.005 pH units in the whole pH range examined. Protonation constants of the ligand and the overall stability constants (β_{pqr}, where p, q and r represent the number of metal, ligand and proton in each of the $Cu_pL_qH_r$ stoichiometries, respectively) of the complexes were evaluated by iterative non-linear least squares fit of the potentiometric equilibrium curves through mass balance equations for all the components, expressed in terms of known and unknown equilibrium constants using the computer program SUPERQUAD [42]. The value obtained for sigma (the root mean squared weighted residual), after refinement of the stability constants, was ≤1, which means that the data was fitted within experimental error. The equilibrium constants reported in this work were obtained from fittings that used three titration curves simultaneously (examples of titration curves are included in Supporting information Fig. S1).

2.2.2. Spectroscopic measurements

Anisotropic EPR spectra were recorded in DMSO/H_2O (30%:70% v/v) at 100 K. Preliminary data indicate that EPR spectra in DMSO are comparable to those detected in the mixture DMSO/H_2O 30%:70% (v/v). Cu(II) solutions were prepared from $^{63}CuSO_4 \cdot 5H_2O$ following literature methods [22], dissolving an exact amount of $^{63}CuSO_4 \cdot 5H_2O$ in the mixture DMSO/H_2O 30%:70% (v/v) to obtain a Cu(II) concentration of 1×10^{-3} M. $^{63}CuSO_4 \cdot 5H_2O$ - used to get better resolution of EPR spectra - was prepared from metallic copper (99.3% ^{63}Cu and 0.7% ^{65}Cu) purchased from JV Isoflex.

UV–vis spectrophotometric titrations were carried out with solutions containing NTSC and Cu(II). The NTSC concentration was 3×10^{-5} M (for the ligand alone), 1×10^{-3} M (for Cu(II)–ligand samples) and the metal-to-ligand ratios were 1:1 and 1:2, in 30% (v/v) DMSO/H_2O. The measurements were done in the pH range between 2 and 12 in the λ interval 200–900 nm, using a quartz cell with a path length of 1 cm.

Fluorescence spectra were recorded at room temperature (ca. 25 °C). CD spectra were recorded in the range from 200 to 360 nm with quartz Suprasil® CD cuvettes (1 cm) at room temperature (ca. 25 °C). Each CD spectrum is the result of three accumulations originally recorded in degrees and converted to Δε values, with the spectropolarimeter software. The following acquisition parameters were used: data pitch: 0.5 nm; bandwidth: 1.0 nm; response: 2 s; scan speed: 100 nm/min.

2.3. Binding to HSA

The UV–visible absorption (UV–vis) and the fluorescence spectra were recorded at room temperature. Millipore water was used for the preparation of solutions and TRIS buffer (0.1 M, pH = 7.4) was employed in these experiments. DMSO from Panreac was used for the preparation of the NTSC and $[Cu(LH_3)(OAc)]\cdot H_2O$ stock solutions. The concentration of HSA was determined by UV–vis absorbance using the molar absorption coefficient at 280 nm (36,850 M^{-1} cm^{-1}) [43]. Deffated HSA (Sigma-Aldrich #A3782) was purchased from Sigma and used as received. The stock solutions of the compounds were prepared by dissolution in DMSO and dilution in TRIS buffer; they were used within a few hours. The amount of organic solvent was kept below 1% (v/v). HSA solutions were prepared by dissolution in TRIS buffer and the solutions were allowed to stand for at least 60 min to allow them to equilibrate. During this period, they were gently swirled (strong agitation was avoided). The fluorescence experiments were done using a quartz cuvette of 1 cm path length, using bandwidths of 8 nm in both excitation and emission. Fluorescence titrations were done in which increasing amounts of the compound's stock solution (0.45 mM) were added to the HSA solution (ca. 1.5 μM). UV–vis absorption spectra were collected to correct the data for reabsorption and inner filter effects. [45,46]. The concentrations were selected in order to have absorbance values below 0.2 at the excitation and emission wavelengths. Blank fluorescence spectra (containing everything except the fluorophore, HSA) were measured and subtracted from each sample's emission spectra. The equilibrium was reached within <5 min. This was checked by measuring fluorescence spectra of a HSA: probe 1:1 solution with time (data not shown).

2.4. Binding to DNA

Fluorescence quenching experiments were carried out by adding increasing amounts of NTSC or CuNTSC (0; 30; 60; 90; 120; 150 μM) to DNA – thiazole orange (TO) system (C_{TO} = 2.6 μM, C_{DNA} = 24 μM, 0.1 M Tris-HCl buffer solution, pH = 7.4). Emission spectra were carried out in a 2 mL quartz cuvette with 430 nm excitation light, and emission was measured at 530 nm. The equilibration time was checked by measuring fluorescence spectra during one hour (DNA: probe = 1:1), but no changes were observed, thus, the equilibration time was kept constant between measurements (5 min). Millipore water was used for the preparation of solutions and phosphate buffer saline (PBS, 0.10 M, pH = 7.4) was employed in the experiments. DMSO from Panreac was used for the preparation of the ligand and complex stock solutions (ca. 3.8 mM). Deoxyribonucleic acid sodium salt from calf thymus (CT-DNA) was purchased from Sigma (#D3664). DNA stock solutions were prepared by dissolution in PBS buffer. The concentration of CT-DNA (ca. 2.5 mM) was determined by UV–vis absorbance using the molar absorption coefficient at 260 (6600 M^{-1} cm^{-1}). The UV absorbance at 260 nm and 280 nm of the CT-DNA solution gave a ratio of 1.9, indicating that the DNA was sufficiently free of protein. UV–vis absorption spectra were collected to correct the data for reabsorption and inner filter effects. [44,45]. The concentrations were selected in order to have absorbance values below 0.2 at the excitation and emission wavelengths. The samples for CD measurements were prepared by adding aliquots of the compounds, NTSC or CuNTSC, to a solution (1.5 mL) containing CT-DNA (60 μM), so that different DNA:compound molar ratios were obtained. The DMSO effect on the DNA spectrum was evaluated in a distinct experiment and subsequently the percentage of DMSO was kept below 1.2% (v/v).

2.5. DNA cleavage

Electrophoresis experiments were carried out with pEGFP-C1 (4731 bp) DNA. The cleavage of pEGFP-C1 by NTSC and CuNTSC systems was accomplished by mixing in the following order: 1 μL of 5 mM Tris-HCl (pH 7.5 containing 5 mM NaCl) buffer, various concentrations (0.00; 0.025; 0.05; 0.10; 0.15; 0.20 mM) of NTSC or $[Cu(LH_3)(OAc)]\cdot H_2O$ and 1 μL of pEGFP-C1 (0.25 μg/μL; 10 mM Tris-buffer, pH 8.0). After mixing, the solutions were incubated at 37 °C for 10 h. The reactions were quenched by addition of EDTA and bromophenol blue and the mixtures were analyzed by gel electrophoresis (0.5% agarose gel). Plasmid cleavage products were quantified and analyzed with the G-BOX Syngene system. The GeneTools software was used to complete gel documentation and analysis. Each concentration was assayed in triplicate in each experiment, and all experiments were repeated at least two times. The results were analyzed using one-way analysis of variance (ANOVA) $p \leq 0.05$.

2.6. Biological activity

In vitro antibacterial activity studies were carried out against Gram-positive bacteria: three strains of *Listeria monocytogenes* (ATCC 19111, ATCC 19112 and ATCC 19115), two strains of *Enterococcus faecalis*

(ATCC 29212 (vancomycin sensitive strain) and ATCC 51299 (vancomycin resistant strain)) and three strains of *Staphylococcus aureus* (ATCC 29737, ATCC 23073 and ATCC 2773), and Gram-negative bacteria: *Salmonella* Typhimurium ATCC 14028 and *Salmonella* Enteritidis ATCC 13076. All bacteria strains were purchased from American Type Culture Collections (MedMark® Europe, France).

In vitro antifungal activity studies were carried out against molds *Geotrichum candidum* 0511, *Alternaria alternate* 0409, *Mucor hiemalis* 0519 and yeasts *Candida albicans DSM* 1386 and *Candida vini* 0008. The strains of fungi were obtained from Collection of Industrial Microorganisms of the Institute of Fermentation Technology and Microbiology ŁOCK 105, Lodz University of Technology.

The bacteria were incubated on the Nutrient Agar (Merck, Germany) for 48 h at 30 °C for *Listeria* species and 48 h at 37 °C for other tested bacteria. The 24 h cultures were inoculated in Nutrient Broth (Merck, Germany) before use. The bacterial counts of the diluted cultures were corrected by adding isotonic NaCl solution to be within the range of 10^6–10^7 colony forming units (CFU).

The molds and yeasts were incubated on the Sabouard Agar (Merck, Germany) for 72 h at 28 °C. The 78 h cultures were inoculated in Sabouard Broth (Merck, Germany) before use. The fungal spore suspensions (or yeast culture) were also corrected by adding isotonic NaCl solution to be within the range of 10^5–10^6 colony forming units (CFU).

Samples of test compounds: $CuCl_2$, NTSC and CuNTSC were dissolved in DMSO to obtain a concentration of 5 mg mL^{-1} and were sterilized by filtration (filter pore width 0.2 μm; Sartorius). Paper disks (∅ = 6 mm) were impregnated with 10 μL of the compound's samples, to obtain a concentration of test compounds of 50.0, 25.0, 12.5, 6.25 μg per disk, and the solvent was allowed to evaporate at room temperature in the dark. The diluted bacterial or fungal test culture (200 μL) was spread on sterile Mueller-Hinton Agar (Merck) plates for bacteria and Sabouard Agar (Merck, Germany) for yeast and molds before placing the sample impregnated paper disks on the plates. A DMSO solution was used as a negative control at the concentration of 20 mg mL^{-1} (this concentration of DMSO did not inhibit the growth of microorganisms) [46]. Vancomycin (Oxoid) was used as positive control for Gram-positive bacteria, kanamycin (Oxoid) for Gram-negative bacteria, at the concentration of 30 μg mL^{-1} each, and nystatin (Oxoid) for the molds at the concentration of 100 UI was used as positive control. After the inhibition, the diameters were measured. As a result, the final diameter of the disk was taken into account (subtracted). The experiments were repeated three times and results were expressed in average values.

2.7. Cell viability assays

Cells (ATCC) were grown in RPMI 1640 medium (A2780) or DMEM containing GlutaMax I (HEK 293) supplemented with 10% fetal bovine serum and were maintained in a humidified atmosphere of 5% CO_2. Cell viability was measured by the colorimetric MTT assay, which assessed active metabolic cells. For a typical assay, cells were seeded in 96-well plates at a density of 1–2 × 10^4 cells/200 μL of appropriate medium and left to incubate approximately 24 h for optimal adherence. Compounds were previously diluted in DMSO and then in the medium. After careful withdrawn of the medium, 200 μL of a serial dilution of compounds in fresh medium were added to the cells (six replicates per compound dilution) and incubation was carried out at 37 °C for 72 h. At the end of treatment the compounds were discarded and the cells were incubated with 200 μL of MTT solution in PBS (0.5 mg mL^{-1}). After 3–4 h at 37 °C the medium was removed and replaced by 200 μL of DMSO to solubilize the purple formazan crystals formed. The percentage of cellular viability was evaluated measuring the absorbance at 570 nm using a plate spectrophotometer (Power Wave Xs, Bio-Tek). The IC_{50} values were calculated with the GraphPad Prism software (version 4.0).

3. Results and discussion

3.1. Potentiometric and spectroscopic studies

The proton dissociation constants (pK_a values) are an important characteristic of any acidic substance, their knowledge being fundamental to understand the ionic composition of the compounds when present in biological media. The chemical or biological activity of acidic compounds depend on their degree of ionization, and accurate knowledge of the dissociation/ionization constants of any particular substance is a prerequisite for the understanding of its mechanism of action both in chemical and biological processes. Therefore, the proton-dissociation processes of NTSC were determined by pH-potentiometric titrations. Due to its low solubility in water, a mixture of DMSO and water DMSO/water 30%:70% (v/v) was used. Such amount of DMSO in the solvent mixture is suitable for aqueous solution equilibrium studies [47]. It allowed dissolution of NTSC at the concentration levels necessary for pH-potentiometric titrations (i.e. 1×10^{-3} or 2×10^{-3} M). Noteworthy, the NTSC can exist in two tautomeric forms (Scheme 1) as it was also described for other thiosemicarbazones [48].

The formation of different protonated NTSC species and the corresponding pK_a values were determined in the studied pH-range (2 − 12). This compound contains four possible dissociable protons, as depicted in Scheme 2.

The proton dissociation constants determined by pH-potentiometry are listed in Table 1 and a species distribution diagram is presented in Fig. 1. Taking into account the pK_a values of the parent ligand – naringenin – the first dissociable proton probably corresponds to the deprotonation of C7–OH group with $pK_{a1} = 7.51$, the second to the C4′–OH with $pK_{a2} = 8.45$ and the third to the deprotonation of $N_{hydrazinic}H$ moiety with $pK_{a3} = 9.19$, in which the negative charge is mainly transferred to the S atom via the thione–thiol tautomeric equilibrium (Scheme 1). The highest pK_a value, $pK_{a4} = 9.96$, is expected to correspond to the proton of the C5–OH moiety, as found for naringenin and other flavonoids [49–51] and Schiff bases of flavanones [22]. The dissociation of these two last protons occurs in a similar pH range, and therefore the pK_a values determined are not much different. It can be inferred that the insertion of thiosemicarbazide moiety into ring C of the naringenin molecule has no relevant effect on the values of pK_{a1} and pK_{a2}, (Table 1). A difference is found in the pK_{a4}, assigned to the C5–OH group, which reflects the different nature of the two compounds and the resonances established in ring A. On the other hand the pK_{a3} of the dissociable –CSNH– proton (9.19) is lower than that found for thiosemicarbazide ($pK_a = 10.24$) [52] and other thiosemicarbazones (e.g. triapine 10.86) [47]. Nevertheless, it is not straightforward to identify which of these two moieties will deprotonate first, the difference between pK_{a4} and pK_{a3} being rather small.

The acid-base properties of NTSC were also investigated by UV–vis absorption titrations in the same pH range as in potentiometry. The electronic absorption spectra of NTSC in the UV region should display at least two sets of bands. The first one at 250–260 nm, attributed to π → π* transitions from the aromatic rings, and the second one at 325–390 nm assigned to n → π* transitions from the azomethine and thioamide functions, overlapped in the same envelope [53]. Representative spectra for NTSC and distinct protonated species present as a function of pH are shown in Fig. 1. As DMSO absorbs in the 240–280 nm range, the bands corresponding to the π → π* transitions cannot be accessed. As a consequence of the progressively more extended conjugated electronic system in NTSC, the deprotonation steps are accompanied by changes in the absorption bands and it is assumed that five distinct absorbing species are formed due to the successive release of protons. Indeed, red shifts and a progressive decrease in the intensity of the bands at ~330 nm are observed upon NTSC deprotonations (Fig. 1). The proton dissociation processes nearly overlap each other, and only fully protonated or deprotonated forms dominate at acidic (pH < 6) or strong alkaline solutions (pH > 11.5), respectively.

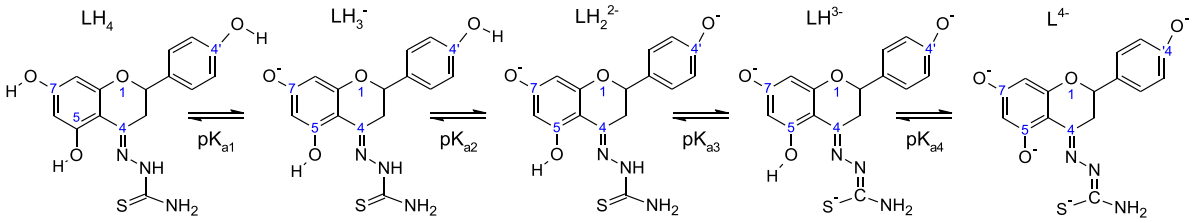

Scheme 2. Proposed dissociation steps of NTSC.

Thiosemicarbazones containing oxygen, nitrogen and sulfur as donors have been extensively studied [54]. In most of the complexes the thiosemicarbazone moiety coordinates to the metal ion in the Z-configuration through the thione/thiol sulfur atom and the azomethine nitrogen atom [55]. The coordination capacity of thiosemicarbazones can be further increased if the ligand contains additional donor moieties in positions suitable for chelation (Fig. 2).

Thiosemicarbazones are basically bidentate with N,S donor set, adequate to coordinate to metal ions, forming a 5-membered chelate ring of a partially conjugate character, and this particular structural characteristic seems to be essential for biological activity [56]. Their biological properties/activity can be modified by introduction of moieties that can participate in π-π interactions and/or hydrogen bonding with biomolecules, e.g. DNA or proteins [57]. This is the case of the NTSC thiosemicarbazone (Fig. 2).

The complex formation process of NTSC with Cu(II) was studied by pH potentiometry in 30% (v/v) DMSO/H_2O solvent mixture. The experimental titration data indicated that NTSC is an efficient metal ion binder in a wide pH range, being able to keep the metal ion in solution at ligand to metal molar ratios of 1 and 2 in the whole pH range 2–12. The overall stability constants of the complexes were determined via pH titrations, also considering the proton dissociation constants of the ligand determined in the absence of the metal ion (Table 1). The best fittings of the titration curves were obtained using the set of K_a and β_{pqr} values listed in Tables 1 and 2 and the species distribution curves of the Cu(II)-NTSC systems are shown in Fig. 3.

The NTSC can act as a tridentate ligand. In acidic medium at 1:1 (L:M) ratio an anchoring site for the Cu(II) ion may be the thione moiety. Upon increasing the pH it is very likely that the binding of the metal ion occurs in a cooperative manner to the azomethine nitrogen and the oxygen from C5–O^- group (Scheme 3). The ligand donor atoms are kept in the whole pH range studied as it is supported by the spectroscopic studies.

It can be seen in Fig. 3 that different protonated species appear upon changing the pH, the complexation processes starting below pH 2. It is not surprising that in spite of the relatively high pK_a values of the NTSC ionisable groups, the protons are displaced at much lower pH ranges in the presence of Cu(II), and Cu-complexes with various protonated forms of the ligand are formed as pH is increased. Similar differences were observed for phenols, flavonoids and their hydrazone derivatives under metal chelation conditions [22,58]. Upon increasing the pH in solutions with 1:1 M ratio the ligand deprotonation at C5–OH and the simultaneous Cu(II) binding via two chelating rings is promoted (Scheme 3). The $CuLH_3^+$ stoichiometry corresponds to the (O^-, N, S) donor atom set with the C7–OH, C4′–OH and $N_{hydrazinic}H$ moieties fully protonated. The next stoichiometry, $CuLH_2$, which predominates at pH around 7 probably corresponds to the same coordination mode of NTSC, but with the C7–OH group deprotonated and the C4′-OH protonated. However, other binding sets cannot be excluded, namely through the (O^-, N, S^-) donor atom set and both C7–OH and the C4′-OH groups protonated, due to the possibility of the thiol-thione tautomerism in the ligand. Above pH 8 the stepwise formation of $CuLH^-$ and CuL^{2-} species occurs. They only differ in the protonation state of the ligand (Scheme 3), the coordination mode being similar. In these complexes the thiolate moiety (—S^-), instead of the thione (=S), is involved in the binding to Cu(II). Taking into account the EPR data (see below), the deprotonation of a coordinated H_2O molecule, forming an OH^- ligand, is not probable. The best fitting of the data above pH 11 was obtained assuming the formation of species with the stoichiometry $Cu_2L_2H_{-2}$. These could correspond to dinuclear/oligomeric/polymeric species coordinated through thiol sulfur and probably OH^- moieties (Fig. 4), which may globally be designated as $Cu_nL_nH_{-n}$ (or $CuLH_{-1})_n$. The formation of polymeric species was also found in other Cu(II)-thiosemicarbazone systems [54]. The presence of counter ions such as Cl^- or NO_3^- has no effect on the spectral parameters giving further support to the hypothesis that the bridging moieties are OH^- groups, not Cl^- or NO_3^- (Fig. S2).

In solutions containing a 2:1 M ratio of NTSC:Cu(II) the species distribution diagram differs and complexes with CuL_2H_n stoichiometries predominate (with n = 6 to 0) (Fig. 3b). Upon increasing the pH, the first bis-chelated Cu(II)-complex is CuL_2H_6 which is neutral (Scheme 4), and upon further deprotonation all stoichiometries correspond to negatively charged complexes. The binding to Cu(II) is probably accomplished through oxygen, nitrogen and sulfur (O^-, N, S) derived from C5–OH, N^1 azomethine and C^3–S moieties, respectively. Each species can be distinguished by the protonation state of the ligand, similarly to the mono-ligand complexes.

Complex formation can be further confirmed by UV–vis absorption spectroscopy (Table 2, Figs. S3 and S4). The spectra recorded in Cu(II)-NTSC systems exhibit bands in the λ ranges 320–470 and 520–750 nm (Figs. S3 and S4, ligand:Cu(II) ratio 1:1 and 2:1, respectively). The absorptions in the 320–470 nm range have been assigned to n → π*

Table 1
The proton dissociation constants ($\log\beta_{LHr}$) of NTSC in DMSO/H_2O 30:70 *v*/v (standard deviations are in parentheses) (25.0 °C, I = 0.10 M (KCl) in 30% (v/v) DMSO/H_2O)) and of naringenin for comparison.

Ligand	Species	$\log\beta_{LHr}$	pK_{a1} C7–OH	pK_{a2} C4′–OH	pK_{a3} $N_{hydrazinic}H$	pK_{a4} 5–OH	Ref.
NTSC	LH_4	35.11(±0.02)	7.51				This work
	LH_3^-	27.60(±0.03)		8.45			
	LH_2^{2-}	19.15(±0.04)			9.19		
	LH^{3-}	9.96(±0.04)				9.96	
Naringenin			7.47	8.49	–	11.12	[49]

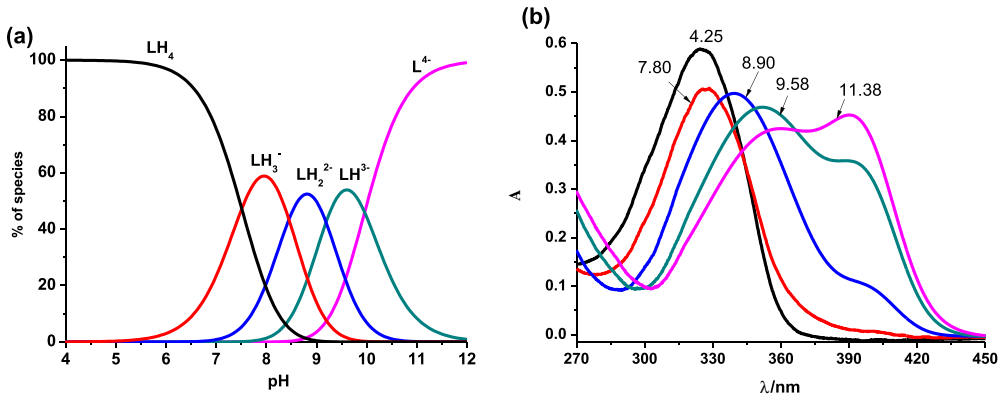

Fig. 1. (a) Species distribution curves of NTSC ($c_{NTSC} = 3 \times 10^{-5}$ M); (b) UV/vis absorption spectra of NTSC recorded at different pH values (the values are indicated by the arrows) ($c_{NTSC} = 3 \times 10^{-5}$ M, I = 0.1 M (KCl), 25 °C) in 30% (v/v) DMSO/H_2O.

transitions from the azomethine and thioamide functions and to LMCT S → d overlapping with O → d, and the absorption in the 520–750 nm range to d–d transitions [59].

The UV–vis titration spectra of solutions containing 1:1 ratio of NTSC:Cu(II) with increasing pH support the presence of the species found by potentiometry. The spectrum recorded at pH 4.00 where $CuLH_3^+$ predominates, shows a broad band at 610 nm corresponding to d-d transitions together with a shoulder at 470 nm attributed to S → Cu/O → Cu charge transfer transitions (Fig. S3b and d). It supports the chelation of copper(II) ions via sulfur, oxygen and nitrogen donor atoms. The visible spectrum at pH 7.03 reveals a broad band with $\lambda_{max} \approx 573$ nm without any clear shoulder (at 450–500 nm), which however may be hidden under the tail of the intense charge transfer band in UV region. This can be ascribed to the $CuLH_2$ species with the same donor atoms as in $CuLH_3^+$. At this pH partial formation of $CuLH^-$ has occurred and a blue shift of the band with respect to the previous one (see Table 2 and Fig. S3b) is due to the possible participation of thiol sulfur in Cu(II) coordination as a result of deprotonation of $N_{hydrazinic}H$ functional moiety in NTSC, as it is observed in other complexes of thiosemicarbazones with Cu(II) [47]. Similar bands are observed at pH 9.30 and 11.09 where, according to the potentiometric results, species with the $CuLH^-$ and CuL^{2-} stoichiometry predominate. The spectral changes are compatible with the same donor set but different protonation state of the NTSC ligand (Table 2).

In alkaline pH the spectrum is characterized by the drastic intensity decrease of the band 565 nm and an appearance of a shoulder at around 650 nm. It can be attributable to changes in the coordination

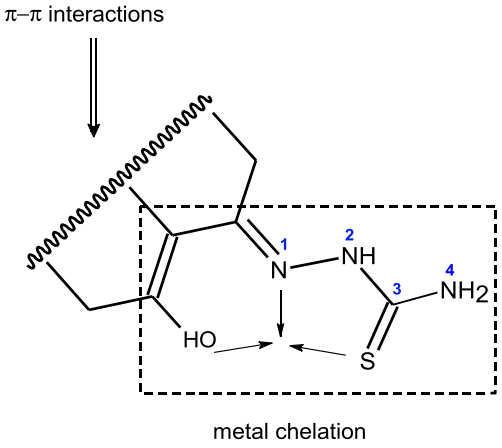

Fig. 2. Expected coordinating donor set in the NTSC.

environment and probably the formation of polymeric forms of complexes with the sulfur and oxygen atoms from thiolato and hydroxylato groups in binding set (yellow-brown color of solution without any precipitation). Such spectra are not observed in DMSO solution (Fig. S3d.) indicating no change of coordination mode with respect to that observed in DMSO/water mixture (30%:70% v/v). The aqueous medium may favor formation of polymeric species through OH^- bridging. The UV spectra are also influenced by changes in pH, supporting the existence of several forms of Cu(II)-complexes with distinct binding sets, thus also with different spectral patterns (Fig. S3a).

The UV–vis spectra in solutions containing 2:1 ratios of NTSC:Cu(II) indicate that the same set of donor atoms [2 × (O^-, N, S/S^-)] can be involved in the binding to Cu(II), as in mono-ligand complexes, with different protonated forms of the NTSC (Table 2). In this system at high pH (> 12) the spectral resolution is drastically reduced, which is probably due to the formation of dimeric or olygomeric species (Fig. S4b) involving the binding of OH^-, as it was found at high pH in solutions with 1:1 ratios.

EPR spectroscopy was used to give further support to the binding modes proposed for each species; this technique is particularly sensitive to changes in the donor atoms/groups coordinated to the paramagnetic Cu(II) centers. In the spectra recorded with solutions containing NTSC:Cu(II) ratio of 1:1 at low pH values, two species are detected in the frozen solution EPR spectra measured at 100 K: $[Cu(Solvent)_6]^{2+}$, where Solvent may be H_2O or DMSO (**Cu(II)** in Fig. 5), and a first Cu-NTSC complex (**I** in Fig. 5 and Fig. S5 of Supporting information). Approximated EPR parameters for **I** are $g_z = 2.210$ and $A_z = 179 \times 10^{-4}$ cm^{-1}, comparable to those found for the solid complex $[Cu(LH_3)(OAc)]\cdot H_2O$, recently characterized ($g_z = 2.180$ and $A_z = 185 \times 10^{-4}$ cm^{-1}), for which [(O^-, N, S); AcO^-] coordination was demonstrated. [26]. The slight increase of g_z and decrease of A_z can be attributed to the presence of a solvent molecule (H_2O or DMSO) instead of an acetate ion in the first coordination sphere of Cu(II). In the first two parallel resonances the superhyperfine coupling between the unpaired electron and the ^{14}N nucleus ($I = 1$) is revealed; in particular, a triplet with intensity ratio 1:1:1 can be observed, denoted by the asterisks in Fig. 5 (it must emphasized that $^{63}CuSO_4$ was used for recording the spectra). An analogous coupling with ^{14}N was recently observed for the Cu(II)-complex formed by the hydrazone hesperetin Schiff base [22]. The value of 14×10^{-4} cm^{-1} for A_z^N is in good agreement with those reported in the literature for other Cu(II) species [60–62]. Therefore, for this species the stoichiometry $CuLH_3^+$ may be assigned with (O^-, N, S) coordination, in agreement with potentiometric and UV–vis data (Figs. 3 and S3).

The deprotonation of $CuLH_3^+$ to give $CuLH_2$ in the pH range 4–5 is not observed by EPR spectroscopy probably because it involves the deprotonation of non-coordinating C7-OH group and does not affect the

Table 2
Overall stability constants ($\log\beta_{Cu_pL_qH_r}$) of Cu(II)-NTSC complexes and spectral parameters in 30% (v/v) DMSO/H_2O (25.0 °C, I = 0.10 M (KCl) (standard deviations are in parentheses).

Complex	$\log\beta_{Cu_pL_qH_r}$	λ_{max} (nm)	g_z	A_z (10^{-4} cm^{-1})	Coordination mode
$CuLH_3^+$	35.55(±0.02)	320, 611	2.210	179	(O^-, N, S); C7-OH; C4′-OH
$CuLH_2$	30.02(±0.02)	333, 573	2.210	179	(O^-, N, S); C7-O^-; C4′-OH or (O^-, N, S^-); C7-OH; C4′-OH
$CuLH^-$	22.00(±0.02)	354, 564	2.200	185	(O^-, N, S^-); C7-O^-; C4′-OH
CuL^{2-}	11.83(±0.02)	370, 565	2.200	185	(O^-, N, S^-); C7-O^-; C4′-O^-
$Cu_2L_2H_{-2}$	2.22(±0.05)	368, 650 sh.	–	–	Dinuclear species
CuL_2H_6	70.78 (±0.02)	320, 627	~2.06	–	2 × (O^-, N, S); 2 C7-OH; 2 C4′-OH
$CuL_2H_5^-$	66.11 (±0.02)	327, 574			2 × (O^-, N, S); C7-O^-; C7-OH; 2C4′-OH
$CuL_2H_4^{2-}$	59.35(±0.03)	335, 564			2 × (O^-, N, S); 2C7-O^-; 2C4′-OH
$CuL_2H_3^{3-}$	50.15(±0.05)	348, 565			(O^-, N, S^-); (O^-, N, S); 2C7-O^-; 2C4′-OH
$CuL_2H_2^{4-}$	40.55(±0.03)	362, 561	2.151	174	2 × (O^-, N, S^-); 2C7-O^-; 2C4′-OH
CuL_2H^{5-}	29.88(±0.04)	368, 561	2.151	174	2 × (O^-, N, S^-); 2C7-O^-; C4′-O^-; C4′-OH
CuL_2^{6-}	19.54(±0.04)	368, 561	2.151	174	2 × (O^-, N, S^-); 2C7-O^-; 2C4′-O^-

binding set. At pH > 7 the deprotonation of hydrazinic N results in the formation of $CuLH^-$ and the coordination switches to (O^-, N, S^-) (**II** in Fig. 5). The presence of a stronger donor in the Cu(II) coordination sphere (S^- vs. S) is indicated by the change of the EPR parameters (g_z = 2.200 and A_z = 185 × 10^{-4} cm^{-1}). In this species the triplet due to the coupling with ^{14}N (indicated by the asterisks in this case too) is not as well resolved as in $CuLH_3^+$ and $CuLH_2$, but an approximated value of ~15 × 10^{-4} cm^{-1} for A_z^N is measurable. Upon the deprotonation of the –OH substituent in position C4′, $CuLH^-$ becomes CuL^{2-}; however, since once again this deprotonation does not involve a coordinating group, EPR parameters remain unchanged till pH 10.5 (see Figs. 5, S5). The decrease of the spectral intensity above pH 10 supports the formation of the oligomeric species $[CuLH_{-1}^{3-}]_n$, here taken as stoichiometry $Cu_2L_2H_{-2}^{6-}$.

When a ligand to metal molar ratio of 2:1 is used, the complexation process starts with the formation of CuL_2H_6 (**I** in Figs. 6 and S6). At pH > 3 the spectra are characterized by a broad band centered at g < 2.06, which indicates the formation of a neutral compound with a not negligible magnetic interaction among the Cu(II) species. This is probably due to partial aggregation/precipitation of the neutral complex upon cooling the solution down to 100 K. For this complex the number of resonances assignable to the superhyperfine coupling between the unpaired electron and the ^{14}N nucleus is larger than three and this confirms that more than one nitrogen is coordinated (these resonances are indicated with the asterisks in Fig. S7). The approximated value of 16 × 10^{-4} cm^{-1} for A_z^N is in good agreement with those reported in the literature for other Cu(II) species [60–62]. The coordination mode of CuL_2H_6 is [2 × (O^-, N, S)]. The pH increasing, and upon the deprotonation of C7-OH, C4′-OH and $N_{hydrazinic}H$ groups, the CuL_2H_6 stoichiometry successively transforms into the anionic species $CuL_2H_5^- \rightarrow CuL_2H_4^{2-} \rightarrow CuL_2H_3^{3-} \rightarrow CuL_2H_2^{4-} \rightarrow CuL_2H^{5-} \rightarrow CuL_2^{6-}$. At pH > 9 the hyperfine coupling pattern, due to the coupling between the unpaired electron and ^{63}Cu appears and, simultaneously, the isotropic band at g < 2.06 disappears. This confirms the formation of different charged species. The EPR parameters g_z = 2.151 and A_z = 174×10^{-4} cm^{-1} can be attributed to a bis-chelated species with a coordination mode [2×(O^-, N, S^-)] [63]. The slight decrease of A_z with respect to **I** and **II** is due to the presence of two donors in the axial position (see also Scheme 3). This species is stable till pH 11.0 (see Fig. 6).

3.2. HSA binding studies

The solution speciation studies showed that NTSC is able to coordinate strongly to Cu(II) and that at physiological pH, under the conditions used in the assay, neutral species $CuLH_2$ predominate (Fig. S8). For a compound to exert its potential biological effect it must reach the cellular targets. In the human body complex processes of drug absorption and bio-distribution will determine the bioavailability of the drug candidate. HSA is one of the plasma proteins involved in the transport of exogenous compounds and therefore the understanding of its interaction with the drug candidates is of utmost importance in the evaluation of their therapeutic potential. HSA is participating in the transport of copper in blood plasma [36,64,65].

HSA presents intrinsic fluorescence due to the presence of tryptophan, tyrosine, and phenylalanine residues. Particularly relevant is Trp214 that can be selectively excited at 295 nm, and its intensity, quantum yield, and wavelength of maximum fluorescence emission is very sensitive to ambient changes. Therefore, HSA fluorescence titrations were done to evaluate the binding ability of both the NTSC ligand and its Cu(II)-complex to HSA. None of the compounds shows fluorescence when excited at 295 nm and thus titrations of the HSA solution with increasing amounts of the compounds were carried out. Figs. 7 and 8

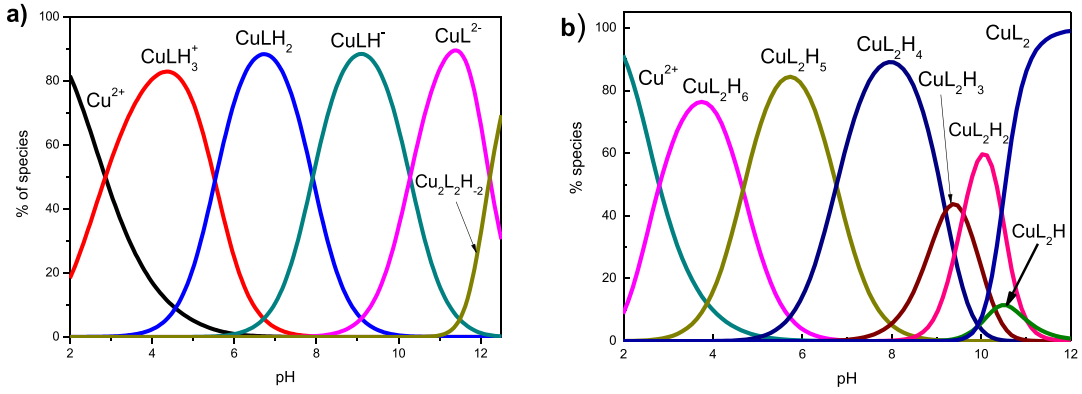

Fig. 3. Concentration distribution of the complexes formed in solutions containing Cu^{2+} and NTSC with different NTSC:Cu ratios: a) 1:1, $c_{Cu(II)} = c_{NTSC} = 1 \times 10^{-3}$ M; b) 2:1 $c_{Cu(II)} = 1 \times 10^{-3}$ M, $c_{NTSC} = 2 \times 10^{-3}$ M (25 °C, I = 0.10 M (KCl) in 30% (v/v) DMSO/H_2O).

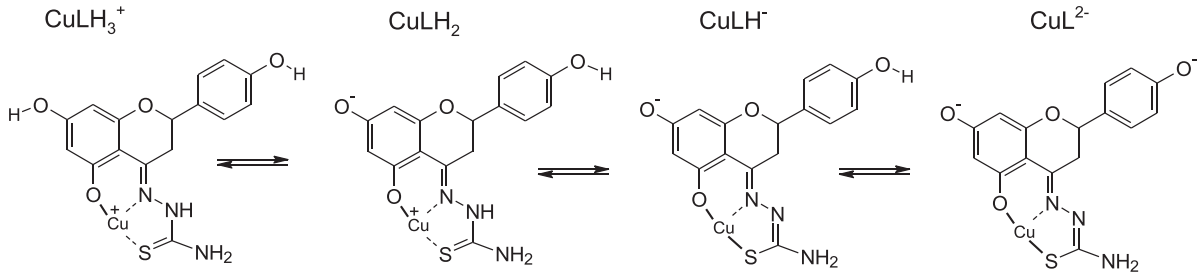

Scheme 3. Ligand donor atoms in the complexes formed in the system with the NTSC:Cu(II) ratio of 1:1.

show HSA fluorescence emission spectra measured in both systems with increasing amounts of the compounds, after subtraction of the blank emission spectra. Addition of the compounds to 1.5 μM solutions of HSA results in strong emission quenching, which is more important for the Cu(II)-complex than for the ligand (88 vs. 62% - see conditions included in Figs. 8 and S9). The fluorescence quenching data was analyzed with the Stern–Volmer equation: $I_0/I = 1 + K_{SV}[Q] = 1 + k_q\tau_0[Q]$, where I_0 and I are the fluorescence emission intensities in the absence and presence of quencher, respectively, and K_{SV}, [Q], k_q and τ_0 stand for the Stern–Volmer quenching constant, the quencher concentration, the bimolecular quenching constant and the average lifetime of the biomolecule without quencher, respectively.

Both Stern-Volmer plots show an upper curvature, particularly evident in the case of the Cu-complex (see Fig. S9). However, in the low quencher concentration range they are roughly linear (Fig. S9b). To evaluate if the quenching is due to binding of the compounds to HSA (static) or to collisional quenching (dynamic), the quenching constant, k_q, was calculated, considering $\tau_0 = 10^{-8}$ s, for the biomolecule [45]. The k_q values obtained were: 4.15×10^{13} and 4.77×10^{13} M^{-1} s^{-1}, for NTSC and CuNTSC, respectively, which are several orders of magnitude higher than the maximum diffusion-limited rate in water [66] indicating that the fluorescence quenching is probably due to binding of the compounds to HSA, thus due to static quenching. We will assume that the mechanism is due to ground-state complex formation, the complex formed being non-fluorescent. The binding constant K_{BD} and the number of binding sites per HSA molecule (n) can be calculated with the equation: $\log [(I_0 - I) / I] = \log K_{BD} + n \times \log[Q]$. Fig. S10 shows the plots and the values obtained for K_{BD} and n are listed in Table 3.

The Stern–Volmer quenching constant K_{SV} obtained by other authors [67] for the interaction of the flavanone naringenin with HSA was 7.8×10^4 M^{-1} at 25 °C, and it decreased linearly with increasing temperature,

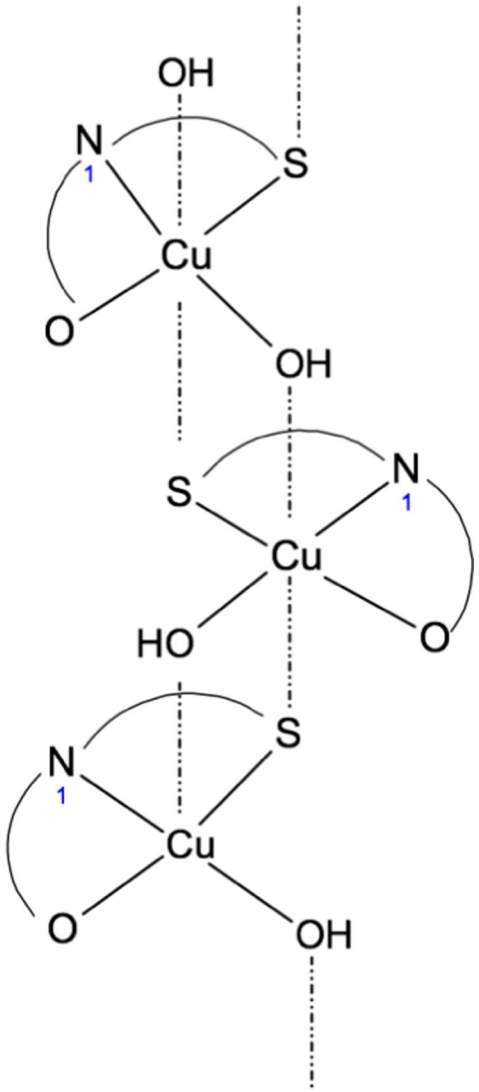

Fig. 4. Proposed structure of oligomeric/polymeric species formed in the Cu(II)-NTSC system for pH > 11, corresponding to stoichiometry $(CuLH_{-1})_n$. The charges are omitted for simplicity.

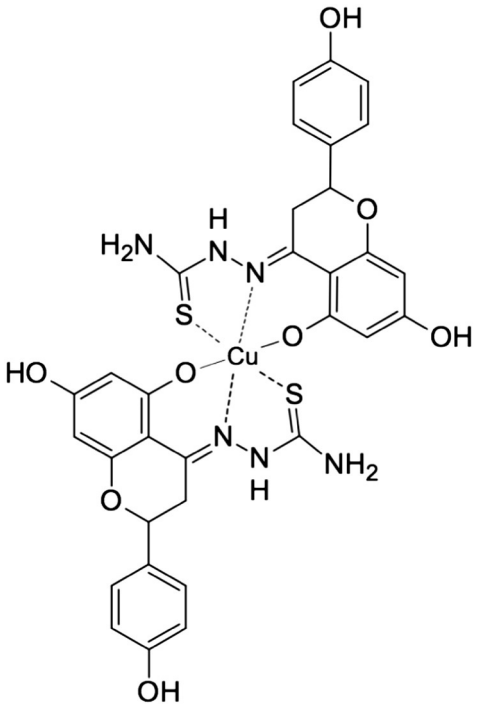

Scheme 4. Proposed binding mode in complexes with the CuL_2H_6 stoichiometry with the C7–OH, C4′–OH and $N_{hydrazinic}H$ moieties protonated.

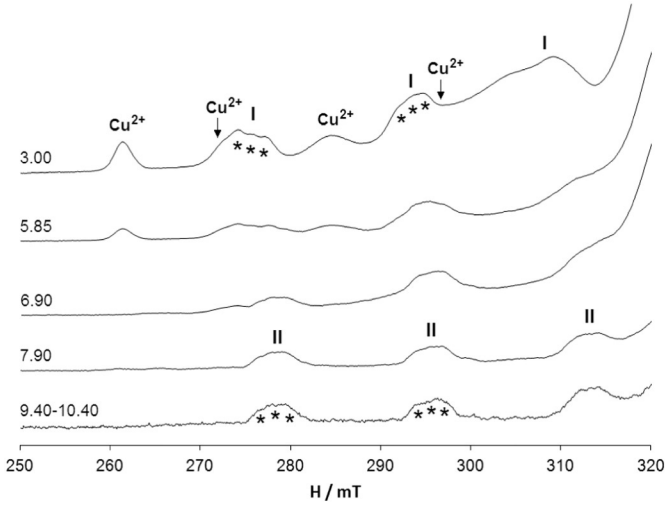

Fig. 5. Low field region of the first derivative X-band anisotropic EPR spectra recorded at 100 K (frozen solutions) on the system with a NTSC:Cu(II) with molar ratio of 1:1 in a mixture DMSO/H_2O 30%:70% (v/v), $c_{Cu(II)} = c_{NTSC} = 1 \times 10^{-3}$ M. With **Cu(II)**, **I** and **II** the resonances of solvated Cu(II) ion, $[CuLH_3]^+/[CuLH_2]$ and $[CuLH]^-/[CuL]^{2-}$ are indicated, and with the asterisks the triplets due to the coupling between the unpaired electron and ^{14}N are marked.

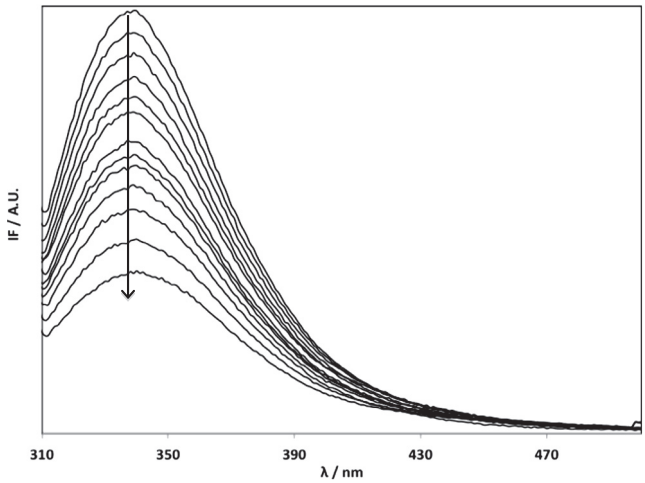

Fig. 7. Fluorescence emission spectra measured for solutions containing HSA (ca. 1.5 μM) and increasing amounts of NTSC (from 0.37 to 8.5 μM) at pH 7.4, after subtraction of blank emission spectra. The arrow indicates increasing NTSC concentration.

confirming also a static quenching mechanism. The value of K_{SV} obtained for the naringenin thiosemicarbazone, NTSC, is 5 times higher than the one measured for naringenin. The K_{SV} constant for naringenin and BSA interaction was even lower (1.66×10^4 M^{-1}) and K_{BD} (1.0×10^5 M^{-1}) was two orders of magnitude lower than that obtained for NTSC [25]. The binding constant of Cu(II) to HSA was determined from equilibrium dialysis experiments; $K_{BD} = 1.5 \times 10^{11}$ M^{-1} [68], and by CD spectroscopy ($\log \beta_1 = 16$ and $\log \beta_2 = 23$) [36] thus being several orders of magnitude higher than those determined for the CuNTSC system. This is due to free Cu(II) ions tightly bind to a specific binding site in HSA at the N-terminus ATCUN motif and to a secondary site, the multi-metal binding site (MBS) [69,70].

At the pH of the experiments the main stoichiometries present in solution are LH_4 and LH_3^- (for NTSC) and $CuLH_2$ (for CuNTSC); it is probable that the binding to HSA involves LH_4 and $CuLH_2$, but that cannot be anticipated with certainty. Globally we can conclude that the Schiff base NTSC binds much more strongly to HSA than the flavanone, and that CuNTSC has even higher affinity for HSA than NTSC. Thus, we anticipate that both the NTSC and CuNTSC may be easily carried by the protein to the drug targets however, and more importantly, the order of magnitude of the K_{BD} values, 10^7–10^8, do not correspond to irreversible binding to the protein [33].

3.3. DNA binding studies

DNA binding is one of the properties looked for in pharmacology – assuming the compound is able to reach the cell nucleus - when evaluating the potential of new anticancer drugs, and hence, the interaction between DNA and such molecules needs to be investigated. Other targets can be intracellular enzymes, membrane transporters, as well as membrane and nuclear receptors and their signaling pathway.

The mode and tendency of the binding of NTSC and CuNTSC with CT-DNA were studied with different spectroscopic methods including fluorescence and circular dichroism. In order to investigate the interaction pattern of the ligand and the complex with DNA fluorescence emission titration analyses were undertaken. The fluorescence intercalator displacement assay has proven to be rapid and accurate for DNA-binding studies. This method is commonly used to study both organic molecules

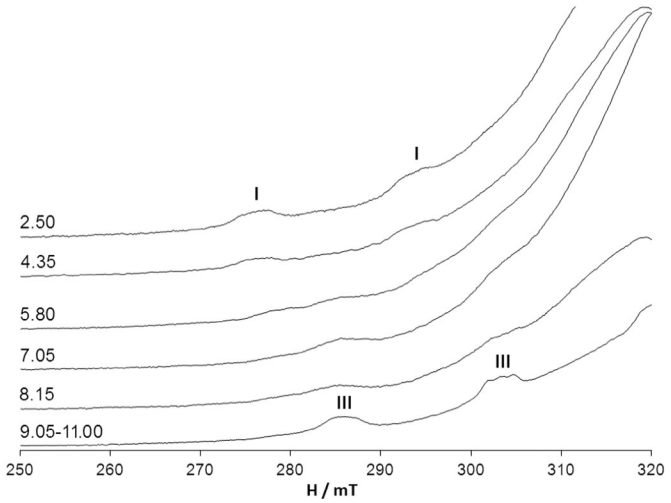

Fig. 6. Low field region of the first derivative X-band anisotropic EPR spectra recorded at 100 K on the system Cu(II)/NTSC with molar ratio 1/2 in a mixture DMSO:H_2O 30%:70% v/v, $c_{Cu(II)} = 1 \times 10^{-3}$ M and $c_{NTSC} = 2 \times 10^{-3}$ M. The resonances of $[CuL_2H_6]^+$ and $[CuL_2H_x]^{(x-6)}$ (with x depending on protonation state of the ligand) are indicated as **I** and **III**.

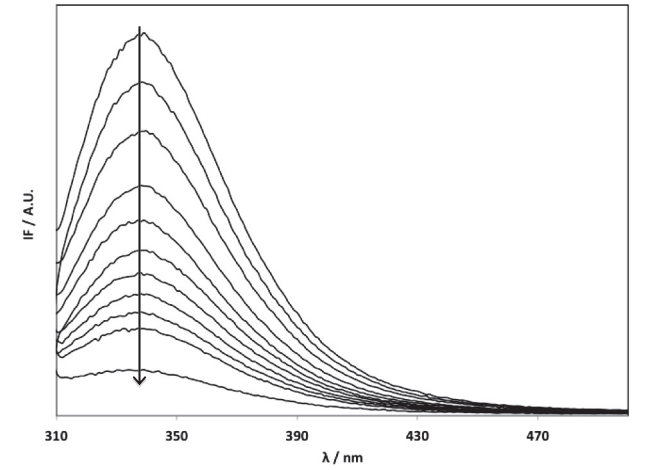

Fig. 8. Fluorescence emission spectra measured for solutions containing HSA (ca. 1.5 μM) and increasing amounts of CuNTSC (from 0.36 to 5.0 μM) at pH 7.4, after subtraction of blank emission spectra. The arrow indicates increasing CuNTSC concentration.

Table 3
Stern–Volmer constant (K_{sv}), quenching rate constant (k_q), binding constant (K_{BD}) and n binding sites for the interaction of NTSC and CuNTSC (Concentration range: 0.35–8 μM) with HSA (1.5 μM), in Tris–HCl (0.1 M, pH 7.4) buffer solutions.

Compound	$10^{-5}K_{SV}$ (M^{-1})	$10^{-13}k_q$ (M^{-1} s^{-1})	10^{-7} K_{BD} (M^{-1})	n
NTSC	4.15 ± 0.07	4.15 ± 0.07	1.02 ± 0.01	1.24 ± 0.02
CuNTSC	4.8 ± 0.3	4.8 ± 0.3	25.2 ± 0.2	1.45 ± 0.04

and metal complexes. It has been shown that thiazole orange (TO) is an excellent dye for these studies since it is safer than ethidium bromide (EB) and binds to double stranded DNA [71]. In this investigation, TO was used for fluorescent intercalator displacement assay. Competitive binding of other molecules with DNA–TO system may result in displacement of TO and decrease of the fluorescence intensity. This fluorescence-based competition technique can provide indirect evidence for binding mode of the compound to DNA. At the pH of the experiments the main stoichiometries very likely present in solution are LH_4 and LH_3^- (for NTSC) and $CuLH_2$ (for CuNTSC). Upon addition of NTSC or CuNTSC, the emission band at 530 nm of the DNA–TO system decreased in intensity with the increase in the concentration of the two compounds, which indicated that the compounds could displace TO from DNA. The spectra are shown in Fig. S11. The resulting decrease in fluorescence was probably caused by TO moving from a hydrophobic environment to an aqueous environment, such a characteristic change being often observed in intercalative DNA interactions [72]. The quenching plots illustrate that the decrease in fluorescence upon addition of NTSC or CuNTSC is in good agreement with the linear Stern–Volmer equation. In the plots of I_0/I versus [Q], K_q (Stern-Volmer quenching constant) [72] is given by the ratio of the slope to the intercept (Fig. S11). The K_q values for the ligand and Cu(II) complex are $4.77(\pm 0.14) \times 10^3$ and $1.79(\pm 0.75) \times 10^4$ M^{-1}, respectively. The value of the apparent binding constant, $K_{app,}$ of the studied compounds was calculated from the equation $K_{app,\ compound} \times [\text{compound}] = K_{app,TO} \times [\text{TO}]$, where $K_{app,TO}$ is the apparent binding constant of TO assumed to be 3×10^6 M^{-1} [73], $K_{app,\ compound}$ is the apparent binding constant of NTSC or CuNTSC to DNA ($K_{app,\ NTSC} = 6.15 \times 10^4$ M^{-1}, $K_{app,\ CuNTSC} = 9.70 \times 10^5$ M^{-1}, respectively), [TO] is the concentration of TO used and [compound] is the concentration of NTSC or CuNTSC at 50% quenching. The data show that the interaction of the Cu(II)-complex with DNA is stronger than that of the free ligand, which is consistent with the absorption spectral results [26] and CD spectral characteristics (see hereafter). Since these changes indicate only one kind of quenching process, it may be concluded that the both compounds bind to DNA via the same mode i.e. partial intercalation, since their apparent binding constants are of the order characteristic for rather moderate intercalators [74].

The binding ability of the NTSC and its Cu-complex to CT-DNA was also evaluated by CD spectroscopy. DNA is chiral, having characteristic CD spectra in the 200–300 nm range, which depends on its conformation. Thus, the CD signal in the UV range allows the detection of conformational changes, damage and/or its cleavage. CT-DNA shows a spectrum typical for right-handed B-form consisting of a positive band centered at 275 nm, attributed to base stacking, and a negative one at 245 nm due to right-handed helicity. Solutions of DNA (ca. 60 μM) were mixed with NTSC or CuNTSC at different molar ratios (from DNA: compound 1:0.25 to 1:1) and the CD spectra measured (Fig. 9). Naringenin used in the synthesis of NTSC was expected to be a racemic compound, however, one of the enantiomers is present in higher amount than the other, as both the NTSC and its Cu-complex present CD bands below 360 nm. Thus, the spectra of NTSC and CuNTSC in the absence of DNA were also measured and are included in the figures for comparison.

Addition of the compounds to DNA leads to a decrease in the intensity of both DNA bands, but changes are much more pronounced in the negative band associated to helicity. Since the compounds present absorptions in the same region of the positive band, their effect is more difficult to rationalize. However, a strong decrease in the intensity of the negative band, accompanied with a red shift is clearly observed. This type of changes has been associated with partial DNA unwinding [75]. Binding of both compounds to CT-DNA was previously established by UV–vis titrations [26] as well as the binding constants for the process, which showed higher affinity for the Cu-complex, when compared to NTSC. The same behavior is observed here, since for the same molar ratio the decrease in the intensity of the helicity band is more pronounced for the Cu-complex. Since no induced CD bands are observed, which usually accompany intercalation of the compounds into the DNA base pairs [75], we propose that besides partial intercalation, electrostatic and hydrogen bonding interactions are also operating. The changes observed in Fig. 9 for the higher amounts of either NTSC or

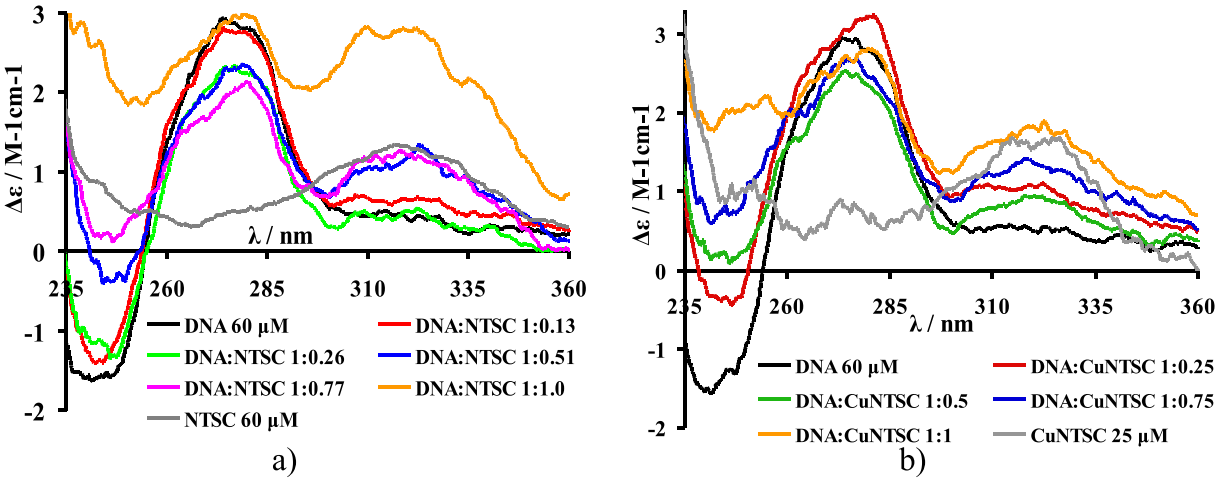

Fig. 9. CD spectra measured for solutions containing DNA (60 μM) in the absence and presence of NTSC (a) and CuNTSC (b); the molar ratios are indicated in the figure. The Δε values of the spectra of the solutions containing CT-DNA were calculated based on its concentration in each solution. The spectra of NTSC and CuNTSC in PBS (0.1 M, pH = 7.4, 1% DMSO) were included for comparison, and are included in differential molar absorbance values (ΔA). Optical path: 1 cm.

CuNTSC are probably due to partial cleavage of CT-DNA, apparently more important in the case of NTSC (see also below).

3.4. Cleavage of pEGFP-C1 DNA

The biological activity of compounds is often related to their ability to cleave DNA. They may bind to DNA either specifically or sequence independent and cleave one or both strands by either a radical or a hydrolytic pathway, the latter being similar to that of natural nucleases [76–79]. Strand cleavage of the naturally occurring supercoiled DNA (Form I SC) may lead either to an open circular relaxed form (Form II OC) upon single strand cleavage or to a linear form (Form III) upon double strand cleavage. The efficiency of NTSC and CuNTSC to cleave pEGFP-C1 DNA was evaluated using gel electrophoresis in the absence of any external reagent or light. Both the ligand and the complex $CuLH_2$ are capable to cleave double stranded DNA (dsDNA) at physiological pH and room temperature. When pEGFP-C1 plasmid DNA was incubated with the compounds, the form I (SC) of the plasmid was hydrolyzed to the form II (OC). The extent of DNA cleavage was quantified and the results are depicted in Fig. S12 (SI).

On the basis of the results we can conclude that the trend of the cleavage efficiencies of NTSC and CuNTSC is similar up to the concentration of 150 μM although quantitative changes in the percentages of OC form are lower for the complex. It seems that the complexation reduces the NTSC cleavage action up to the concentration of 150 μM and that of the Cu(II) ion in the whole range of the concentration (Fig. S12). Therefore, in the experiments with CuNTSC, we expect that the complex is mainly responsible for dsDNA cleavage, not free Cu(II) ions. As no additional reagents like H_2O_2 or ascorbic acid were used in the experiments, we suggest a hydrolytic pathway of DNA cleavage as proposed in previous publication for other Cu-complexes [22,32].

3.5. Effect of NTSC and CuNTSC on microorganisms

The biological activities of the NTSC ligand, its copper complex CuNTSC and $CuCl_2$ were screened in antimicrobial tests with several Gram-positive and Gram-negative bacteria, as well as in antifungal tests with several molds and yeasts. Gram-positive bacteria have different susceptibility to the test compounds in contrast to Gram-negative, which are quite resistant to them (data presented in Supporting information Table S1). In the present experimental conditions the selected fungi were resistant to all the compounds, this data being presented only in the Supporting information (Table S2). From the results presented in Tables 4 and 5 we can indicate the following trend of the compound's impact on the inhibition of bacterial growth: *Listeria monocytogenes* ATCC 19111 > *Enterococcus faecalis* ATCC 51299 > *Staphylococcus aureus* ATCC 23073 > *Staphylococcus aureus* ATCC 2773. It should be noted, however, that the effect of vancomycin is always higher than that of the tested compounds. The strongest effect of the complex was seen for *Listeria monocytogenes* ATCC 19111 and *Enterococcus faecalis* ATCC 51299. *Listeria monocytogenes* ATCC 19115 is characterized by higher susceptibility to NTSC than to CuNTSC. The complex probably diminishes the NTSC effectiveness towards bacterial growth. The reason for this could be the changes of NTSC structural features after the complexation which can affect its activity to the bacteria. Such structural rearrangements may enable selective interaction between the Cu-complex and putative binding sites on target proteins. It could lead to restrict the ligand penetration into cells.

Staphylococcus aureus ATCC 29737 reveals a weak effect at the highest concentration of Cu(II) ions but no inhibition effect under the action of NTSC or CuNTSC. *Staphylococcus aureus* ATCC 23073 depicts a similar impact of the action of Cu(II) ions as that observed in *Listeria monocytogenes* ATCC 19111; on the other hand *Staphylococcus aureus* ATCC 2773 has a similar effect to that of *Staphylococcus aureus* ATCC 29737. The CuNTSC displays a significant influence on ATCC 2773 and ATCC 23073. The NTSC shows no impact on all these bacterial strains as well as on *Enterococcus faecalis*. *Salmonella* Typhimurium ATCC and *Salmonella* Enteritidis ATCC are the only examples in this study resistant to the actions of Cu(II), NTSC or CuNTSC.

We can hypothesize that NTSC, due to formation of a lipophilic complex with Cu(II) (at pH around 7, the non-charged $CuLH_2$ is the most relevant stoichiometry) could translocate Cu(II) across cell membranes and exert antimicrobial activity, as it has been documented for other Cu(II)-complexes [80]. The increased lipophilic character of CuNTSC may favor its interaction with the cell constituents, resulting in

Table 5
Antibacterial activity of test compounds against *Enterococcus faecalis* and *Staphylococcus aureus* bacteria.

CuNTSC [μM]			$CuCl_2$ [μM]			Vancomycin [μM]
0.103	0.051	0.026	0.373	0.186	0.093	0.021
Enterococcus faecalis ATCC 29212 Inhibition zone diameters [mm]						
0.0	0.0	0.0	1.5 ± 0.3	0.0	0.0	15.0 ± 0.2
Enterococcus faecalis ATCC 51299 Inhibition zone diameters [mm]						
8.0 ± 1.0	4.0 ± 0.5	0.0	3.5 ± 0.5	1.5 ± 0.2	0.0	5.0 ± 0.1
Staphylococcus aureus ATCC 29737 Inhibition zone diameters [mm]						
0.0	0.0	0.0	1.5 ± 0.1	0.0	0.0	16.0 ± 0.3
Staphylococcus aureus ATCC 23073 Inhibition zone diameters [mm]						
6.0 ± 1.5	4.2 ± 0.3	0.0	5.0 ± 0.9	4.5 ± 0.6	0.0	8.0 ± 0.5
Staphylococcus aureus ATCC 2773 Inhibition zone diameters [mm]						
3.0 ± 0.5	1.0 ± 0.0	0.0	2.5 ± 0.9	0.0	0.0	10.0 ± 1.3

Table 4
Antibacterial activity of test compounds against *Listeria monocytogenes* bacteria.

CuNTSC [μM]			NTSC [μM]			$CuCl_2$ [μM]			Vancomycin [μM]
0.103	0.051	0.026	0.145	0.072	0.036	0.373	0.186	0.093	0.021
Listeria monocytogenes ATCC 19111 Inhibition zone diameters [mm]									
7.2 ± 1.2	7,0 ± 0.9	3.5 ± 0.5	0.0	0.0	0.0	5.0 ± 0.2	4.2 ± 0.1	0.0	17.0 ± 1.2
Listeria monocytogenes ATCC 19112 Inhibition zone diameters [mm]									
4.0 ± 1.0	0.0	0.0	2.0 ± 0.8	0.0	0.0	2.0 ± 0,7	0.0	0.0	25.5 ± 2.5
Listeria monocytogenes ATCC 19115 Inhibition zone diameters [mm]									
5.0 ± 1.0	4.0 ± 0.5	0.0	7.0 ± 0.6	5.0 ± 1.0	1.0 ± 0.5	2.0 ± 0.1	0.0	0.0	20.0 ± 3.0

interference with the normal cell processes [81,82]. Taking into account literature data it can be assumed that the antibacterial action of the CuNTSC complex is due to, on one side to its action as a Cu ionophore (carrier of Cu ions across cell membranes), as well as direct inhibitor of respiratory chain, as it was shown for other thiosemicarbazone Cu-complexes [83–85].

Summing up, although structural aspects of the ligand, Cu(II) and of the complex may be relevant to the mechanism of action of the copper complex, the effectiveness of Cu(II)-species depends heavily on the physiology of the bacteria (different susceptibility was observed in the selected group of Gram-positive and none in Gram-negative). This is probably also connected to the ability of the target bacterium to tolerate Cu and, additionally, very likely to the susceptibility of the respiratory chain to direct inhibition by the complex [86,87]. For instance, CuNTSC may be reduced and destabilized by the action of respiratory enzymes e.g. NADH dehydrogenase. Then the liberated copper ions could inflict damage through adverse interactions with critical thiols or iron sulfur clusters of respiratory or metabolic proteins, as reported elsewhere [88–90].

3.6. Cytotoxicity study

The cytotoxic activity of NTSC, CuNTSC, as well as of naringenin and its Cu(II) complex, were evaluated in cancer and normal cell lines, A2780 and HEK, respectively. The Fig. S13 (SI) shows the concentration-response curves, obtained for the two complexes after 72 h of incubation. It is evident that NTSC and CuNTSC show no cytotoxicity even at a concentration of 100 μM. Both naringenin and NTSC were also non-cytotoxic for these cell lines. While A2780 are ovarian cancer cells, HEK are derived from human embryonic kidney cells. As both NTSC and CuNTSC are capable to cleave dsDNA, we may conclude that the compounds do not reach the nucleus of these cells.

Cytotoxicity studies have been reported for several flavonoids and metal complexes of flavonoids [15,23,25] some of them having been shown to be cytotoxic, others not. Islas et al. [25], in a study testing several flavonoids and their $V^{IV}O$-complexes against lung (A549) and breast (SK-Br-3 and MDA-MB-231) cancer cell lines, observed, as in the present study, IC_{50} values higher than 100 μM, while the $V^{IV}O$(naringenin)$_2$ complex depicted IC_{50} values of 73 (SKBr3 cells) and 20 μM (MDAMB231 cells). The cytotoxicity of naringenin and Cu(naringenin)$_2$ (and other flavonoids and their Cu-complexes) was evaluated against human cancer cell lines hepatocellular carcinoma (HepG-2), gastric carcinomas (SGC-7901), and cervical carcinoma (HeLa) [19]. Not much details are given but globally naringenin and Cu(naringenin)$_2$ were not very active, and only in the case of the HepG-2 cell line Cu(II) enhanced significantly the inhibitory rate compared to naringenin.

Therefore, the low cytotoxicity of Cu(naringenin)$_2$ determined in the present study agrees with earlier work reported for this system. This and the low cytotoxicity of CuNTSC against the HEK cell line may be considered positive results since it suggests that the CuNTSC compound can be used as an antimicrobial agent without showing toxicity against normal cells. Further tests with several other types of cell lines should be carried out.

4. Conclusions

Equilibrium solution studies carried out on the NTSC and Cu(II)-NTSC systems in DMSO/water mixture have revealed the formation of different forms of the ligand and the complexes with coordination modes supported by UV–vis absorption and EPR data. NTSC has four protons that may dissociate in the pH range 2–12, and globally the results obtained in the work indicate that NTSC is a potent tridentate ligand for Cu(II) ions. The binding sets of the complexes formed in Cu(II)-NTSC systems, as the pH or the molar ratios of ligand to metal are varied, were determined. Several mono- and bis-ligand complexes in different protonation states were identified.

The emission spectral results show that the interaction of the Cu-complex with DNA is stronger than that of the free ligand and it is concluded that both compounds bind DNA via partial intercalation. Circular dichroism spectra measured with solutions containing CT-DNA and either NTSC or CuNTSC confirm that both compounds interact with this biomolecule, producing changes mainly in the negative band at ~245 nm, normally associated with DNA helicity, but also in the positive band at ~275 nm, normally attributed to base stacking. In experiments concerning the cleavage potential towards plasmid DNA, the results showed that Cu(II) complexation with NTSC protects DNA from the nuclease action of free Cu(II) ions.

Fluorimetric experiments with human serum albumin (HSA), based on the quenching effect of the Trp214 residue, showed that the CuNTSC compound exhibits stronger binding to HSA than NTSC. The binding constants obtained, $1.0 \times 10^7\ M^{-1}$ (NTSC) and $2.5 \times 10^8\ M^{-1}$ (CuNTSC), indicate that the compounds may be transported in blood plasma by HSA, and that they do not bind irreversibly to this protein.

Naringenin, NTSC, Cu(naringenin)$_2$ and CuNTSC complexes depict IC_{50} values against the cancer A2780 and normal KEK cell lines higher than 100 μM, thus they may be considered non-toxic, at least towards these two cell lines. Growth inhibition studies with several selected fungi indicated no effect, at least in the experimental conditions used. In contrast, antibacterial growth inhibition studies showed that the effectiveness of NTSC or CuNTSC depends on the type of bacteria tested. For example, while no inhibition was found against *Staphylococcus aureus* ATCC 29737, a strong effect is demonstrated for *Listeria monocytogenes* ATCC 19111 and *Enterococcus faecalis* ATCC 51299. These results suggest that if NTSC or CuNTSC are found useful as bactericidal agents, they will probably be quite selective for this purpose, not affecting much the normal cells.

Acknowledgement

The authors thank the financial support from Statute Funds No. I28/DzS/9184, the Fundação para a Ciência e a Tecnologia, the program Investigador FCT, project UID/QUI/00100/2013 and RECI/QEQ-QIN/0189/2012.

Appendix A. Supplementary data

Supplementary data to this article can be found online at http://dx.doi.org/10.1016/j.jinorgbio.2016.09.014.

References

[1] J.S. Casas, M.S. García-Tasende, J. Sordo, Coord. Chem. Rev. 209 (2000) 197–261.
[2] K. Brodowska, E. Łodyga-Chruscinska, Flavonoids and antioxidant, in: J.N. Govil, S. Bhattacharya, G. Kaushik (Eds.), Recent Progress in Medicinal Plants, 40, Studium Press (India) Pvt. Ltd., New Delhi 2014, pp. 36–61.
[3] J. Kang, L. Zhuo, X. Lu, H. Liu, M. Zhang, H. Wu, J. Inorg. Biochem. 98 (2004) 79–86.
[4] C. Kanadaswami, L.T. Lee, P.P. Lee, J.J. Hwang, F.C. Ke, Y.T. Huang, M.T. Lee, In Vivo 5 (2005) 895–909.
[5] B.A. Graf, P.E. Milbury, J.B. Blumberg, J. Med. Food 8 (2005) 281–290.
[6] S.J. Habtemariam, J. Nat. Prod. 60 (1997) 775–778.
[7] N. Sugihara, A. Takayuki, M. Ohnishi, K. Furuno, Free Radic. Biol. Med. 27 (1999) 1313–1323.
[8] X. Zheng, W.D. Meng, Y.-Y. Xu, J.G. Cao, F.L. Qinga, Bioorg. Med. Chem. Lett. 13 (2003) 881–884.
[9] M.M. Kamel, H.I. Ali, M.M. Anwar, N.A. Mohameda, M. Soliman, Eur. J. Med. Chem. 45 (2010) 572–580.
[10] J. Benítez, A. Cavalcanti de Queiroz, I. Correia, M. Amaral Alves, M.S. Alexandre-Moreira, E.J. Barreiro, L. Moreira Lima, J. Varela, M. González, H. Cerecetto, V. Moreno, J. Costa Pessoa, D. Gambino, Eur. J. Med. Chem. 62 (2013) 20–27.
[11] M. Fernández, L. Becco, I. Correia, J. Benítez, O.E. Piro, G.A. Echeverria, A. Medeiros, M. Comini, M.L. Lavaggi, M. González, H. Cerecetto, V. Moreno, J. Costa Pessoa, B. Garat, D. Gambino, J. Inorg. Biochem. 127 (2013) 150–170.
[12] B. Demoro, R.F.M. Almeida, F. Marques, C.P. Matos, L. Otero, J. Costa Pessoa, I. Santos, A. Rodríguez, V. Moreno, J. Lorenzo, D. Gambino, A.I. Tomaz, Dalton Trans. 42 (2013) 7131–7146.
[13] D.S. Kalinowski, P. Quach, D.R. Richardson, Future Med. Chem. 1 (2009) 1143–1151.
[14] G. Pelosi, TOCRYJ 3 (2010) 16–28.

[15] L. Naso, E.G. Ferrer, L. Lezama, T. Rojo, S.B. Etcheverry, P.A.M. Williams, J. Biol. Inorg. Chem. 15 (2010) 889–902.
[16] E.G. Ferrer, M.V. Salinas, M.J. Correa, L. Naso, D.A. Barrio, S.B. Etcheverry, L. Lezama, T. Rojo, P.A.M. Williams, J. Biol. Inorg. Chem. 11 (2006) 791–801.
[17] L.G. Naso, E.G. Ferrer, N. Butenko, I. Cavaco, L. Lezama, T. Rojo, S.B. Etcheverry, P.A.M. Williams, J. Biol. Inorg. Chem. 16 (2011) 653–668.
[18] L. Naso, M. Valcarcel, P. Villacé, M. Roura-Ferrer, C. Salado, E.G. Ferrer, P.A.M. Williams, New J. Chem. 38 (2014) 2414–2421.
[19] M. Tan, J. Zhu, Y. Pan, Z. Chen, H. Liang, H. Liu, H. Wang, Bioinorg. Chem. Appl. 1–9 (2009).
[20] Y. Li, Z.Y. Yang, M.F. Wang, J. Fluoresc. 20 (2010) 891–905.
[21] Y. Li, Z.Y. Yang, Inorg. Chim. Acta 362 (2009) 4823–4831.
[22] E. Lodyga-Chruscinska, M. Symonowicz, A. Sykula, A. Bujacz, E. Garribba, M. Rowinska-Zyrek, S. Oldziej, E. Klewicka, M. Janicka, K. Krolewska, M. Cieslak, K. Brodowska, L. Chruscinski, J. Inorg. Biochem. 143 (2015) 34–47.
[23] I.E. León, J.F. Cadavid-Vargas, I. Tiscornia, V. Porro, S. Castelli, P. Katkar, A. Desideri, M. Bollati-Fogolin, S.B. Etcheverry, J. Biol. Inorg. Chem. 20 (2015) 1175–1191.
[24] L.G. Naso, L. Lezama, M. Valcarcel, C. Salado, P. Villacé, D. Kortazar, E.G. Ferrer, P.A.M. Williams, J. Inorg. Biochem. 157 (2016) 80–93.
[25] M.S. Islas, L.G. Naso, L. Lezama, M. Valcarcel, C. Salado, M. Roura-Ferrer, E.G. Ferrer, P.A.M. Williams, J. Inorg. Biochem. 149 (2015) 12–24.
[26] K. Brodowska, A. Sykuła, E. Garribba, E. Łodyga-Chruscinska, M. Sójka, Transit. Met. Chem. 41 (2016) 179–189.
[27] J. Costa Pessoa, I. Correia, T. Kiss, T. Jakusch, M.M.C.A. Castro, C.F.G.C. Geraldes, J. Chem. Soc. Dalton Trans. (2002) 4440–4450.
[28] I. Correia, A. Dornyei, T. Jakusch, F. Avecilla, T. Kiss, J. Costa Pessoa, Eur. J. Inorg. Chem. 14 (2006) 2819–2830.
[29] S. Gama, F. Mendes, F. Marques, I.C. Santos, I. Correia, J. Costa Pessoa, I. Santos, A. Paulo, J. Inorg. Biochem. 105 (2011) 637–644.
[30] S. Gama, I. Rodrigues, F. Marques, E. Palma, I. Correia, M.F.N.N. Carvalho, J. Costa Pessoa, A. Cruz, S. Mendo, I.C. Santos, F. Mendes, I. Santos, A. Paulo, RSC Adv. 4 (2014) 61363–61377.
[31] I. Correia, S. Roy, C.P. Matos, S. Borovic, N. Butenko, I. Cavaco, F. Marques, J. Lorenzo, A. Rodríguez, V. Moreno, J. Costa Pessoa, J. Inorg. Biochem. 147 (2015) 134–146.
[32] J. Borowska, M. Sierant, E. Sochacka, D. Sanna, E. Lodyga-Chruscinska, J. Biol. Inorg. Chem. 20 (2015) 989–1004.
[33] F. Kratz, J. Control. Release 132 (2008) 171–183.
[34] T. Jakusch, D. Hollender, É.A. Enyedy, C.S. González, M. Montes-Bayón, A. Sanz-Medel, J. Costa Pessoa, I. Tomaz, T. Kiss, Dalton Trans. (2009) 2428–2437.
[35] J. Costa Pessoa, I. Tomaz, Curr. Med. Chem. 17 (2010) 3701–3738.
[36] D. Sanna, P. Buglyó, A.I. Tomaz, J. Costa Pessoa, S. Borović, G. Micera, E. Garribba, Dalton Trans. 41 (2012) 12824–12838.
[37] T. Mukherjee, J. Costa Pessoa, A. Kumar, A.R. Sarkar, Inorg. Chim. Acta 426 (2015) 150–159.
[38] Y. Zhang, S. Shi, X. Sun, X. Xiong, M. Pengn, J. Inorg. Biochem. 105 (2011) 1529–1537.
[39] G. Gran, Acta Chem. Scand. 4 (1950) 559–577.
[40] H.M. Irving, M.G. Miles, L.D. Pettit, Anal. Chim. Acta 38 (1967) 475–488.
[41] SCQuery, The IUPAC stability constants database, academic software (version 5.5), Royal Society of Chemistry, 1993–2005.
[42] P. Gans, A. Vacca, A. Sabatini, J. Chem. Soc. Dalton Trans. (1985) 1195–1200.
[43] I. Correia, T. Jakusch, E. Cobbinna, S. Mehtab, I. Tomaz, N.V. Nagy, A. Rockenbauer, J. Costa Pessoa, T. Kiss, Dalton Trans. 41 (2012) 6477–6487.
[44] A. Coutinho, M. Prieto, J. Chem. Educ. 70 (1993) 425–428.
[45] B. Valeur, Molecular Fluorescence. Principles and Applications, Wiley, Weinheim, 2001.
[46] C. Piccirillo, S. Demiray, A.C. Silva Ferreira, M.E. Pintado, P.M.L. Castro, Ind. Crop. Prod. 43 (2013) 562–569.
[47] É.A. Enyedy, N.V. Nagy, É. Zsigó, C.R. Kowol, V.B. Arion, B.K. Keppler, T. Kiss, Eur. J. Inorg. Chem. (2010) 1717–1728.
[48] E. Kohli, R. Arora, R. Kakkar, Can. Chem. Trans. 2 (2014) 327–342.
[49] K. Brodowska, Biotechnol. Food Sci. 77 (2013) 45–53.
[50] A. Farajtabar, F. Gharib, Chem. Pap. 67 (2013) 538–545.
[51] K. Lemańska, H. Szymsiak, B. Tyrakowska, R. Zielinski, A.E.M.F. Soffers, I.M.C.M. Rietjiens, Free Radic. Biol. Med. 31 (2001) 869–881.
[52] M.M. Hamada, A.-H.M. Shallaby, O. El-Shafai, A.A. El-Asmy, Transit. Met. Chem. 31 (2006) 522–529.
[53] J.G. Da Silva, A.A. Recio Despaigne, S.R. Louro, C.C. Bandeira, E.M. Souza-Fagundes, H. Beraldo, Eur. J. Med. Chem. 65 (2013) 415–426.
[54] T.S. Lobana, R. Sharma, G. Bawa, S. Khanna, Coord. Chem. Rev. 253 (2009) 977–1055.
[55] A.I. Matesanz, P. Souz, Mini-Rev. Med. Chem. 9 (2009) 1389–1396.
[56] M. Liu, T. Lin, A.C. Sartorelli, Prog. Med. Chem. 32 (1995) 1–35.
[57] J.W. Steed, D.R. Turner, K.J. Wallace, Core Concepts in Supramolecular Chemistry and Nanochemistry, John Wiley & Sons, Ltd, Chichester, UK, 2007.
[58] R.C. Hider, Z.D. Liu, H.H. Khodr, Metal chelation of polyphenols, in: L. Packer (Ed.), Methods in Enzymology, 335, Academic Press, San Diego 2001, pp. 190–194.
[59] J. García-Tojal, A. García-Orad, J.L. Serra, J.L. Pizarro, L. Lezama, M.I. Arriortua, T. Rojo, J. Inorg. Biochem. 75 (1999) 45–54.
[60] R. Klement, F. Stock, H. Elias, H. Paulus, P. Pelikán, M. Valko, M. Mazúr, Polyhedron 18 (1999) 3617–3628.
[61] S. Thakurta, J. Chakraborty, G. Rosair, J. Tercero, M.S. El Fallah, E. Garribba, S. Mitra, Inorg. Chem. 47 (2008) 6227–6235.
[62] A. Ray, S. Mitra, A.D. Khalaji, C. Atmani, N. Cosquer, S. Triki, J.M. Clemente-Juan, S. Cardona-Serra, C.J. Gómez-García, R.J. Butcher, E. Garribba, D. Xu, Inorg. Chim. Acta 363 (2010) 3580–3588.
[63] U. Sakaguchi, A.W. Addison, J. Chem. Soc. Dalton Trans. (1979) 600–608.
[64] C. Harford, B. Sarkar, Acc. Chem. Res. 30 (1997) 123–130.
[65] W. Bal, J. Christodoulou, P.J. Sadler, A. Tucker, J. Inorg. Biochem. 70 (1998) 33–39.
[66] J.R. Lakowicz, Principles of Fluorescence Spectroscopy, 2nd Edition Springer Science & Business Media, 2013.
[67] B. Tu, Y. Wang, R. Mi, Y. Ouyang, Y.-J. Hu, Spectrochim. Acta A 149 (2015) 536–543.
[68] J. Masuoka, J. Hegenauer, B.R. Van Dyke, P. Saltman, J. Biol. Chem. 268 (1993) 21533–21537.
[69] C.A. Blindauer, J. Lu, A.J. Stewart, P.J. Sadler, T.J.T. Pinheiro, Biochem. Soc. Trans. 36 (2008) 1317–1321.
[70] T. Peters Jr., All About Albumin: Biochemistry, Genetics, and Medical Applications, Academic Press, San Diego, CA, 1996.
[71] D.L. Boger, W.C. Tse, Bioorg. Med. Chem. 9 (2001) 2511–2518.
[72] Y.B. Zeng, N. Yang, W.S. Liu, N. Tang, J. Inorg. Biochem. 97 (2003) 258–264.
[73] D. Monchaud, C. Allain, M.P. Teulade-Fichou, Bioorg. Med. Chem. Lett. 16 (2006) 4842–4845.
[74] J. Qian, X. Ma, J. Tian, W. Gu, J. Shang, X. Liu, S. Yan, J. Inorg. Biochem. 104 (2010) 993–999.
[75] N.C. Garbett, P.A. Ragazzon, J.B. Chaires, Nat. Protoc. 2 (2007) 3166–3172.
[76] E.L. Hegg, J.N. Burstyn, Coord. Chem. Rev. 173 (1998) 133–165.
[77] J.L. Tian, L. Feng, W. Gu, G.J. Xu, S.P. Yan, D.Z. Liao, Z.H. Jiang, P. Cheng, J. Inorg. Biochem. 102 (2007) 196–202.
[78] J. Qian, W. Gu, H. Liu, F.X. Gao, L. Feng, S.P. Yan, D.Z. Liao, P. Cheng, Dalton Trans. 10 (2007) 1060–1066.
[79] J. Chen, X.Y. Wang, Y.G. Zhu, J. Lin, X.L. Yang, Y.Z. Li, Y. Lu, Z.J. Guo, Inorg. Chem. 44 (2005) 3422–3430.
[80] R.A. Festa, M.E. Helsel, K.J. Franz, D.J. Thiele, Chem. Biol. 21 (2014) 977–987.
[81] B. Murukan, K. Mohanan, J. Enzyme Inhib, Med. Chem. 22 (2007) 65–70.
[82] P.K. Panchal, H.M. Parekh, P.B. Pansuriya, J. Enzyme Inhib. Med. Chem. 21 (2006) 203–209.
[83] A. Speer, T.B. Shrestha, S.H. Bossmann, R.J. Basaraba, G.J. Harber, S.M. Michalek, M. Niederweis, O. Kutsch, F. Wolschendorf, Antimicrob. Agents Chemother. 57 (2013) 1089–1091.
[84] M. Haeili, C. Moore, C.J. Davis, J.B. Cochran, S. Shah, T.B. Shrestha, Y. Zhang, S.H. Bossmann, W.H. Benjamin, O. Kutsch, F. Wolschendorf, Antimicrob. Agents Chemother. 58 (2014) 3727–3736.
[85] K.Y. Djoko, B.M. Paterson, P.S. Donnelly, A.G. McEwan, Metallomics 6 (2014) 854–863.
[86] S. Kerscher, S. Drose, V. Zickermann, U. Brandt, Results Probl. Cell Differ. 45 (2008) 185–222.
[87] L.A. Schurig-Briccio, T. Yano, H. Rubin, R.B. Gennis, Biochim. Biophys. Acta 1837 (2014) 954–963.
[88] M. Suwalsky, B. Ungerer, L. Quevedo, F. Aguilar, C.P. Sotomayor, J. Inorg. Biochem. 70 (1998) 233–238.
[89] Z. Vardanyan, A. Trchounian, Cell Biochem. Biophys. 57 (2010) 19–26.
[90] L. Macomber, J.A. Imlay, Proc. Natl. Acad. Sci. U. S. A. 106 (2009) 8344–8349.